JACS
JOURNAL OF THE AMERICAN CHEMICAL SOCIETY

COMMUNICATION

pubs.acs.org/JACS

Facile Mechanosynthesis of Amorphous Zeolitic Imidazolate Frameworks

Thomas D. Bennett,[†] Shuai Cao,[†] Jin Chong Tan,[†] David A. Keen,[§] Erica G. Bithell,[†] Patrick J. Beldon,[#] Tomislav Friscic,[#] and Anthony K. Cheetham*[,†]

[†]Department of Materials Science and Metallurgy, University of Cambridge, Cambridge CB2 3QZ, U.K.

[§]ISIS Facility, Rutherford Appleton Laboratory, Harwell Oxford, Didcot OX11 0QX, U.K.

[#]Department of Chemistry, University of Cambridge, Cambridge CB2 1EW, U.K.

Supporting Information

ABSTRACT: A fast and efficient mechanosynthesis (ball-milling) method of preparing amorphous zeolitic imidazolate frameworks (ZIFs) from different starting materials is discussed. Using X-ray total scattering, N_2 sorption analysis, and gas pycnometry, these frameworks are indistinguishable from one another and from temperature-amorphized ZIFs. Gas sorption analysis also confirms that they are nonporous once formed, in contrast to activated ZIF-4, which displays interesting gate-opening behavior. Nanoparticles of a prototypical nanoporous substituted ZIF, ZIF-8, were also prepared and shown to undergo amorphization.

Considerable attention has been given to zeolitic imidazolate frameworks (ZIFs), a subfamily of metal−organic frameworks (MOFs) in which imidazolate-derived ligands (Im=$C_3H_3N_2^-$) and metal (M^{2+}) ions form open-framework [$M(Im)_2$] structures adopting zeolitic topologies.[1−3] These numerous porous structures have been the subject of interest focusing on their sorption and catalytic properties,[4,5] the development of ZIF thin films and membranes being particularly promising from an application perspective.[6] Significant progress has been made in addressing the lack of understanding of the mechanical properties of this exciting class of materials,[7] with particular reference to inter- and intrafamily structure−property relationships.[8,9]

Conventional ZIF synthesis relies on the solvothermal reaction between the imidazolate ligand and a metal source at temperatures in the range 80−140 °C, though some can be produced under ambient conditions. The mechanosynthesis of ZIFs and MOFs in general using liquid-assisted grinding (LAG)[10] represents a notable advance in this area,[11,12] being a faster, inexpensive, and cleaner route to larger sample quantities than other methods. While advances in synthetic techniques for novel framework topologies and compositions are ongoing, new ZIF-based materials are also being reported which derive from existing frameworks. The synthesis and characterization of thermally amorphized ZIFs (a_T-ZIFs), for example, offers unique opportunities to combine the functional tunability of MOFs with amorphous phase properties, potentially opening routes to photoluminescent and optically active glasses.[13,14] The application of hydrostatic pressure to ZIFs yields similarly interesting novel materials, such as porous amorphous ZIFs,[15] while also being utilized for effective pore evacuation without collapse.[16] The *reversible* amorphization of a ZIF was recently reported,[17] demonstrating reversible sorption characteristic modification.

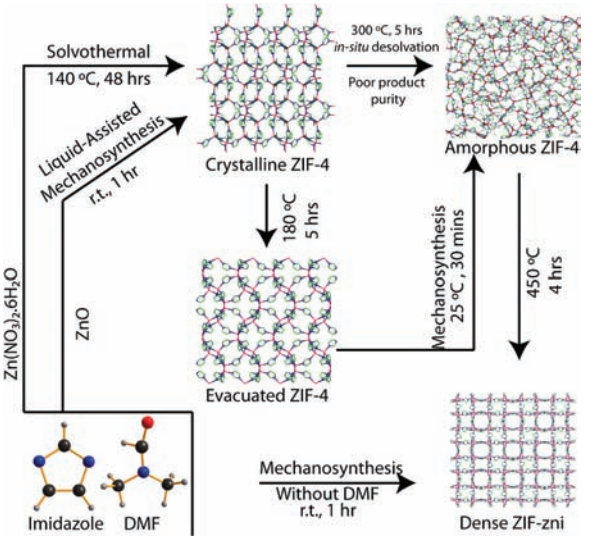

Figure 1. Synthesis of ZIF-4, *a*-ZIF-4, and ZIF-zni using hydrothermal and ball-milling techniques. Not only is mechanosynthesis faster, cheaper, and more straightforward, but it also greatly reduces the crystalline impurities frequently found in a_T-ZIFs. The hydrogen atom bonded to the nitrogen in the imidazole molecule has been omitted to show the deprotonated imidazolate linker present in the crystalline frameworks.

In the present work, we report that mechanosynthesis can *irreversibly* amorphize crystalline ZIFs (Figure 1). The structure and properties of the materials produced (a_m-ZIFs) are compared and contrasted to those produced by thermal amorphization. We also report that nanocrystals of porous ZIF-8 with substituted imidazolate ligands can be amorphized by milling.

ZIF-1 [$Zn(Im)_2$] and the structurally polymorphic ZIF-3 and -4 were produced and evacuated according to the previously reported synthetic procedures (SI-1). The materials were ball-milled without solvent for 30 min at room temperature (see SI for further details). The only product obtained from each reaction was amorphous (Figure 2). This is faster than the thermal amorphization of ZIFs, which, like the related aluminosilicates,

Received: June 30, 2011
Published: August 17, 2011

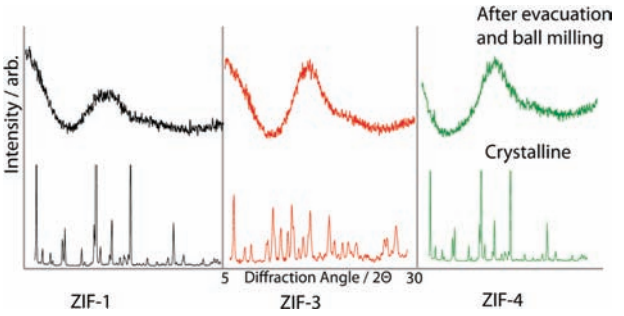

Figure 2. Uncorrected X-ray diffraction patterns for crystalline ZIF-1, -3, and -4 (bottom) produced by solvothermal synthesis, and amorphous phases (top) as produced by mechanosynthesis.

Table 1. Pycnometric Density Measurements for the Crystalline (Solvent-Containing) ZIFs, the Temperature-Amorphized ZIFs, and the ZIFs Amorphized by Milling (Densities in g cm^{-3})

	crystalline[a]	a_T-ZIFs [a]	a_m-ZIFs
ZIF-1	1.4828(6)	1.575(4)	1.581(5)
ZIF-3	1.1763(20)	1.572(4)	1.575(3)
ZIF-4	1.4616(5)	1.576(4)	1.570(2)

[a] Data for crystalline phases (solvent containing) and a_T-ZIFs from ref 14.

is strongly time dependent.[18] Typically heating at 300 °C for at least 2 h is required to effect complete amorphization. Powder X-ray diffraction (PXRD) analysis was repeated over a month to confirm the irreversibility of the transition. Whereas small crystalline impurities (e.g., untransformed starting materials) are common in the a_T-ZIFs, no such impurities were observed in the a_m-ZIFs. The ease with which amorphization can be achieved with ball-milling, compared with heating or hydrostatic pressure, suggests that shear deformation may be important in the mechanism.

While the formation of ZIF-4 and the dense, most thermodynamically stable ZIF-zni (which may also be formed upon further heating of ZIF-4 via a_T-ZIF, see Figure 1) directly from imidazolate and metal salt precursors by *liquid-assisted* mechanosynthetic means has been reported previously,[12] attempts to synthesize the amorphous phase directly from these precursors were unsuccessful. Similarly, milling crystals of ZIF-4 did not result in ZIF-zni formation, although ZIF-zni was observed upon heating the a_m-ZIFs to 450 °C, as found with the a_T-ZIFs (Figure 1). The pycnometric densities of the a_m-ZIFs are very close to one another and to those of the a_T-ZIFs (Table 1).

Total scattering data on a_m-ZIF-1, -3, and -4 were collected at room temperature using Ag X-ray radiation (λ = 0.561 Å) (SI-2) and compared to those obtained previously for a_T-ZIF-4. The X-ray total scattering structure factors $S(Q)$ and the corresponding pair distribution functions (PDFs) $G(r)$ are shown in Figure 3. It is clear from the PDFs that the short-range orderings (SROs) of the a_m-ZIFs are identical to one another and to that of the a_T-ZIF-4 (Figure 3a), the limit of SRO being taken as the nearest-neighbor inter-zinc distance of 6 Å. Slight variations at very low r can be explained by the low statistics in $S(Q)$ at high Q. The same features in the SROs have been observed across all crystalline and amorphous ZIFs studied. Above the 6 Å limit in the a_m-ZIFs, inspection of the PDFs reveals only the existence of

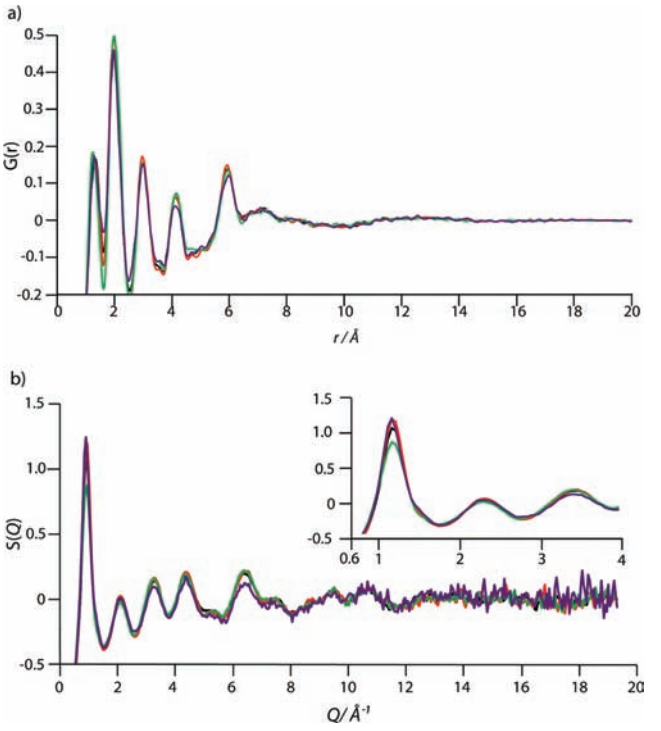

Figure 3. X-ray total scattering data measured for the a_m-ZIFs. (a) Pair distribution function $G(r)$ calculated via Fourier transform of $S(Q)$ for a_m-ZIF-1 (black), a_m-ZIF-3 (red), a_m-ZIF-4 (green), and a_T-ZIF-4 (purple). (b) X-ray total scattering function $S(Q)$. Inset: Low-Q region of $S(Q)$.

a broad, low-intensity feature at ~12 Å. This feature is also observed in the a_T-ZIFs but not in the crystalline phases.

The similarity of the $S(Q)$ traces at low Q (inset, Figure 3b) also indicates that the a_m-ZIFs have very similar medium-range orderings (MROs), which extends farther than the next-nearest-neighbor interatomic distance. The first sharp diffraction peak (FSDP) is generally accepted to be a good indicator of MRO in covalently bonded glasses,[19,20] the full width at half-maximum (FWHM) of the FSDP being used to determine a rough measure of the MRO in silica glass (the coherence length, L).[21] In previous work on the structure of a_T-ZIFs, we calculated an L value of >10 Å (the value found in the case of silica glass). Despite small differences in the intensity of the FSDP, the FWHM is largely unchanged from that observed previously, again suggesting repetition of interatomic distances of >10 Å throughout a significant volume of the a_m-ZIFs, though not in a periodic manner characteristic of long-range crystalline order. At this stage, no differences in the MROs between the a_T-ZIFs and a_m-ZIFs can be detected, suggesting that very similar amorphous materials are produced from the two different synthetic approaches.

To further characterize the amorphous ZIFs, N_2 sorption analysis was performed on the a_m-ZIFs and a_T-ZIF-4 at 77 K. The results confirm that the materials have no nanoporosity but are similar to the dense ZIF-zni prepared by solvothermal reaction (Figure 4a). Differences in the apparent surface areas of the two classes of amorphous material were apparent, however, with the a_m-ZIFs having greater Brunauer–Emmett–Teller (BET) surface areas than a_T-ZIF-4 (Table S1).

Characterization of samples of a_m-ZIF-4 and a_T-ZIF-4 by transmission electron microscopy (TEM) confirms that the typical

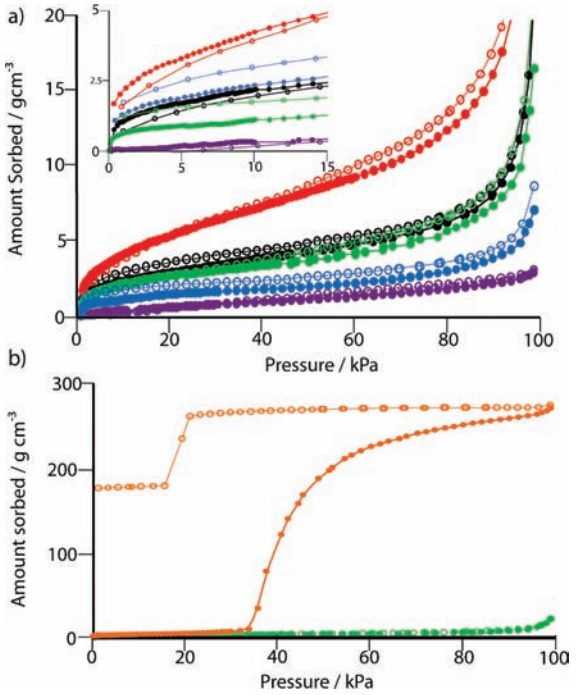

Figure 4. (a) N_2 sorption isotherms for a_m-ZIF-1 (black), a_m-ZIF-3 (red), a_m-ZIF-4 (green), a_T-ZIF-4 (purple), and ZIF-zni (blue). Closed circles indicate adsorption, while open circles indicate desorption. Inset: Sorption at low pressures, clearly indicating the lack of microporosity (pore size of up to 2 nm) in the five amorphous materials. (b) N_2 isotherm for ZIF-4 crystalline (orange) compared to a_m-ZIF-4 (green). A step in the adsorption isotherm is clearly observed around 35 kPa, the gate "closing" at ~20 kPa on desorption.

particle size in a_m-ZIF-4 is significantly smaller than in the thermally amorphized sample. The wider distribution of particle sizes, along with the greater predominance of small particles in a_m-ZIF-4, is evident from the TEM images (Figure S2). Particle sizes in a_T-ZIF-4 were typically ~4−10 μm, with few smaller particles, whereas the particle size in a_m-ZIF-4 was typically <4−5 μm, with a substantial population of particles as small as 50 nm in diameter.

Nitrogen gas sorption analysis was also performed on a sample of activated crystalline ZIF-4. The N_2 sorption isotherm shown in Figure 4b reveals a gate-opening behavior not unlike those already reported in ZIF-7 and -8.[22,23] The porosity of ZIF-4 only becomes evident at ~35 kPa, where a rapid increase in N_2 sorption from 10 to 260 cm^3g^{-1} is indicative of a transition to a more porous structure. The sorption-induced transition is reminiscent of ZIF-8, where a more open phase appears at 2 kPa; the gate-opened ZIF-8 is related to the ambient phase by a simple rotation of the imidazolate ligands.[24] While investigations to determine the identity of the gate-opened structure of ZIF-4 are ongoing, the higher pressure of the effect is consistent with concerted imidazolate rotation being inhibited by the lower solvent-accessible volume and higher density of the structure (Table S2). Though the total N_2 adsorbed by the system was unremarkable (260 compared to 400 cm^3 g^{-1} for ZIF-8) and the BET surface area relatively small (300 compared to 1630 m^2 g^{-1}),[3] the result is of specific relevance to work on capturing harmful gaseous species (e.g., I_2, CO_2) in MOFs. For example, gate-opening of the type now found in ZIF-4, -7, and -8 could provide a mechanism for trapping adsorbed species.

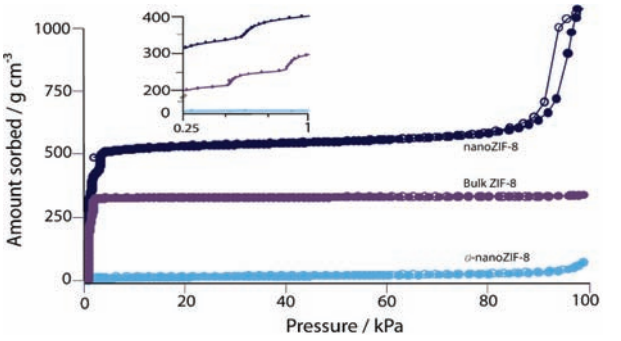

Figure 5. N_2 sorption isotherms for bulk ZIF-8, nano-ZIF-8, and a_m-nanoZIF-8. Closed circles indicate adsorption, while open circles indicate desorption. Inset: Sorption at low pressures.

Many of the porous ZIFs which display the most promising sorption capacities contain substituted imidazolate ligands and can exhibit thermal stabilities up to 500 °C since they do not amorphize upon heating. ZIF-8 [$Zn(mIm)_2$] (mIm = 2-methylimidazolate) provides such an example. We prepared activated nanocrystals of this prototypical ZIF (nanoZIF-8) according to previous procedures[25] and subjected the sample to an identical ball-milling treatment as done for the unsubstituted ZIFs. The average particle size, in line with prior investigations of ZIF-8 nanoparticles,[25] was ~60 nm, as estimated from the broadening of the Bragg reflections and by TEM observations (Figure S3). The resultant purely amorphous product (*a*-nanoZIF-8) (Figure S1) was stable over at least one month at room temperature under atmospheric exposure. Total scattering data on a_m-nanoZIF-8 were collected and compared to those obtained for a_m-ZIF-1 (Figure S4). While the SRO is similar to that observed in all other ZIFs, the MRO appears to be different from that of the unsubstituted amorphous phases. Reverse Monte Carlo modeling (e.g., ref 13) is underway to investigate this further. A sample of bulk crystalline ZIF-8 showed partial amorphization on ball-milling (Figure S1) but contained a significant amount of crystalline impurity attributed to zinc oxide.

Gas pycnometry on the three activated samples (ZIF-8, nanoZIF-8, and a_m-nanoZIF-8) revealed similar pycnometric densities for the two crystalline samples of 1.42(2) and 1.45(1) g cm^{-3}, along with the expected densification of the structure on amorphization (1.52 g cm^{-3}). Subsequent N_2 sorption analysis confirmed that, like the previous amorphous frameworks, a_m-nanoZIF-8 was not nanoporous. In line with previous results, and as expected given the smaller particle size (Figure S3b), a larger BET surface area for nanoZIF-8 of 1630 m^2 g^{-1} was attained, compared to 1006 m^2 g^{-1} for the bulk sample. The maximum uptake capacity of 1000 cm^3 g^{-1} for nanoZIF-8 was reduced to 312 cm^3 g^{-1} for the bulk sample (Figure 5). By contrast, the BET surface area of the a_m-nanoZIF-8 was 56 m^2 g^{-1}, and the maximum uptake was only 70 cm^3 g^{-1}, both attributed to external surfaces of the particles.

In conclusion, this is a first study that not only presents a faster and more efficient route to amorphous ZIFs but also develops a technique for the synthesis of amorphous ZIFs containing substituted imidazolate ligands The characterization of each of the a_m-ZIFs as nonporous represents an advance in our knowledge on the amorphous MOF domain. Further work on the ball-milling-induced amorphization of substituted ZIFs (which are resistant to thermal amorphization) is warranted in order to

elucidate the underlying mechanisms. In addition, an exploration of amorphization with samples that have not been evacuated could have interesting consequences.

■ ASSOCIATED CONTENT

Supporting Information. Synthesis details, materials characterization, and supplementary data. This material is available free of charge via the Internet at http://pubs.acs.org.

■ AUTHOR INFORMATION

Corresponding Author
akc30@cam.ac.uk

■ ACKNOWLEDGMENT

The authors thank the ERC and the EPSRC for funding to T.D.B., S.C., J.C.T., E.G.B., and A.K.C., and Emma Barney for technical assistance with the total scattering measurements. P.J.B. thanks the EPSRC via the Cambridge NanoDTC for funding. T.F. acknowledges the Herchel Smith fund for a Research Fellowship.

■ REFERENCES

(1) Tian, Y. Q.; Cai, C. X.; Ren, X. M.; Duan, C. Y.; Xu, Y.; Gao, S.; You, X. Z. *Chem.—Eur. J.* **2003**, *9*, 5673.
(2) Tian, Y. Q.; Zhao, Y. M.; Chen, Z. X.; Zhang, G. N.; Weng, L. H.; Zhao, D. Y. *Chem.—Eur. J.* **2007**, *13*, 4146.
(3) Park, K. S.; Ni, Z.; Cote, A. P.; Choi, J. Y.; Huang, R. D.; Uribe-Romo, F. J.; Chae, H. K.; O'Keeffe, M.; Yaghi, O. M. *Proc. Natl. Acad. Sci. U.S.A.* **2006**, *103*, 10186.
(4) Banerjee, R.; Furukawa, H.; Britt, D.; Knobler, C.; O'Keeffe, M.; Yaghi, O. M. *J. Am. Chem. Soc.* **2009**, *131*, 3875.
(5) Zakzeski, J.; Debczak, A.; Bruijnincx, P. C. A.; Weckhuysen, B. M. *Appl. Catal., A* **2011**, *394*, 79.
(6) Venna, S. R.; Carreon, M. A. *J. Am. Chem. Soc.* **2010**, *132*, 76.
(7) Tan, J. C.; Cheetham, A. K. *Chem. Soc. Rev.* **2011**, *40*, 1059.
(8) Tan, J. C.; Bennett, T. D.; Cheetham, A. K. *Proc. Natl. Acad. Sci. U.S.A.* **2010**, *107*, 9938.
(9) Bennett, T. D.; Tan, J. C.; Moggach, S. A.; Galvelis, R.; Mellot-Draznieks, C.; Reisner, B. A.; Thirumurugan, A.; Allan, D. R.; Cheetham, A. K. *Chem.—Eur. J.* **2010**, *16*, 10684.
(10) Friščic, T.; Reid, D. A.; Halasz, I.; Stein, R. S.; Dinnebier, R. E.; Duer, M. J. *Angew. Chem., Int. Ed.* **2010**, *49*, 712.
(11) Fernandez-Bertran, J. F.; Hernandez, M. P.; Reguera, E.; Yee-Madeira, H.; Rodriguez, J.; Paneque, A.; Llopiz, J. C. *J. Phys. Chem. Solids* **2006**, *67*, 1612.
(12) Beldon, P. J.; Fabian, L.; Stein, R. S.; Thirumurugan, A.; Cheetham, A. K.; Friscic, T. *Angew. Chem., Int. Ed.* **2010**, *49*, 9640.
(13) Bennett, T. D.; Goodwin, A. L.; Dove, M. T.; Keen, D. A.; Tucker, M. G.; Barney, E. R.; Soper, A. K.; Bithell, E. G.; Tan, J. C.; Cheetham, A. K. *Phys. Rev. Lett.* **2010**, *104*, 115503.
(14) Bennett, T. D.; Keen, D. A.; Tan, J. C.; Barney, E. R.; Goodwin, A. L.; Cheetham, A. K. *Angew. Chem., Int. Ed.* **2011**, *50*, 3067.
(15) Chapman, K. W.; Halder, G. J.; Chupas, P. J. *J. Am. Chem. Soc.* **2009**, *131*, 17546.
(16) Moggach, S. A.; Bennett, T. D.; Cheetham, A. K. *Angew. Chem., Int. Ed.* **2009**, *48*, 7087.
(17) Bennett, T. D.; Simoncic, P.; Moggach, S. A.; Gozzo, F.; Macchi, P.; Keen, D. A.; Tan, J. C.; Cheetham, A. K. *Chem. Commun.* **2011**, *47*, 7983.
(18) Greaves, G. N.; Meneau, F.; Sapelkin, A.; Colyer, L. M.; Gwynn, I. A.; Wade, S.; Sankar, G. *Nat. Mater.* **2003**, *2*, 622.
(19) Uchino, T.; Harrop, J. D.; Taraskin, S. N.; Elliott, S. R. *Phys. Rev. B* **2005**, *71*, 014202.
(20) Elliott, S. R. *Phys. Rev. Lett.* **1991**, *67*, 711.
(21) Lucovsky, G.; Phillips, J. C. *Nanoscale Res. Lett.* **2010**, *5*, 550.
(22) Gucuyener, C.; van den Bergh, J.; Gascon, J.; Kapteijn, F. *J. Am. Chem. Soc.* **2010**, *132*, 17704.
(23) Aguado, S.; Bergeret, G.; Titus, M. P.; Moizan, V.; Nieto-Draghi, C.; Bats, N.; Farrusseng, D. *New J. Chem.* **2011**, *35*, 546.
(24) Fairen-Jimenez, D.; Moggach, S. A.; Wharmby, M. T.; Wright, P. A.; Parsons, S.; Duren, T. *J. Am. Chem. Soc.* **2011**, *133*, 8900.
(25) Huber, K.; Cravillon, J.; Nayuk, R.; Springer, S.; Feldhoff, A.; Wiebcke, M. *Chem. Mater.* **2011**, *23*, 2130.